

1 **Plant functional traits modulate the effects of soil acidification on above- and**
2 **belowground biomass**

3 Xue Feng ¹, Ruzhen Wang ^{1,2}, Tianpeng Li ¹, Jiangping Cai ¹, Heyong Liu ^{1,2}, Hui Li ¹,
4 Yong Jiang ^{1,2,*}

5 ¹Erguna Forest-Steppe Ecotone Ecosystem Research Station, Institute of Applied
6 Ecology, Chinese Academy of Sciences, Shenyang 110016, China

7 ²College of Life Sciences, Hebei University, Baoding 071002, Hebei, China

8

9 * Correspondence: Yong Jiang (jiangyong@iae.ac.cn).

10

11 **Abstract**

12 Atmospheric sulfur (S) deposition has been extensively recognized as a major driving
13 force of soil acidification. However, little is known on how soil acidification influences
14 above- and belowground biomass via altering leaf and root traits.

15 A 3-year elemental S addition were conducted to simulate soil acidification in a meadow.
16 Grass (*Leymus chinensis*) and sedge (*Carex duriuscula*) species were chosen to
17 demonstrate the linkage between plant traits and biomass.

18 Sulfur addition led to soil acidification and nutrient imbalance. For *L. chinensis*, soil
19 acidification decreased specific leaf area but increased leaf dry matter content showing
20 a conservative strategy and thus suppression of aboveground instead of belowground
21 biomass. For *C duriuscula*, soil acidification increased plant height and root nutrients
22 (N, P, S, and Mn) for competing resources by investing more on above- and
23 belowground biomass, *i.e.*, an acquisitive strategy. An overall reduction in community
24 aboveground biomass by 3-33% resulted from the increased soil acidity. While the
25 community root biomass increased by 11-22% as upregulated by higher soil nutrient
26 availability.

27 Our results provide new insights that plant above- and belowground biomass is
28 conditioned by S-invoked acidification and their linkages with plant traits contributed
29 to a deeper understanding of plant-soil feedback.

30 **Keywords:** sulfur addition, soil acidification, meadow grassland, functional traits,
31 plant biomass

32

33 **1 Introduction**

34 Acid deposition as a consequence of anthropogenic activities will have important
35 impacts on terrestrial biodiversity and ecosystem functions and services (Tian and Niu,
36 2015; Clark et al., 2019; Yang et al., 2021). Atmospheric sulfur (S) deposition is one of
37 the main causations of soil acidification, and its contribution is equal to or exceeds that
38 of nitrogen (N) deposition in Asia (Duan et al., 2016; Zhang et al., 2022). Despite large
39 decrease in average S deposition across China over the past decades, it is still very
40 serious in Northeast China and Inner Mongolia (Yu et al., 2017). The northern
41 grasslands of China as an integral part of the Eurasian grassland have experienced
42 severe soil acidification with a significant decline in mean soil pH from 7.84 to 7.21
43 during 1980s- 2000s, while S deposition can undoubtedly accelerate this process (Yang
44 et al., 2012). Therefore, soil acidification has become a major global concern, not only
45 leading to soil nutrient losses but also decreasing the productivity of terrestrial
46 ecosystems (Chen et al., 2013a; Tibbett et al., 2019; Duddigan et al., 2021).

47 In natural ecosystems, sulfur is an essential nutrient in forming plant proteins
48 because it is a constituent of certain amino acids, but S limitation rarely occurs
49 (Vitousek and Howarth, 1991; Garrison et al., 2000). Shifts in plant species and
50 community associated with S deposition were mainly a consequence of soil
51 acidification rather than a S-fertilization effect (Clark et al., 2019). This is because soil
52 pH is a primary regulator of nutrient availability that plant growth and species co-
53 existence rely on (Bolan et al., 2003; Tibbett et al., 2019). For instance, soil acidification
54 inhibits nitrification (Kemmitt et al., 2005), but promotes the release of soil available
55 phosphorus (P), micronutrients and the leaching of soil base cations (Jaggi et al., 2005;
56 Chen et al., 2015; Feng et al., 2019). Evidence from contrived S addition
57 experimentation has shown that aboveground biomass (AGB) decreased with soil
58 acidification, whereas sedges with high acid tolerance revealed the opposite pattern in
59 a subalpine grassland (Leifeld et al., 2013). The acidification-mediated decrease in soil
60 cation concentrations (such as Ca^{2+} and NO_3^-) could increase the relative abundance of
61 acid-tolerant and oligotrophic species (van Dobben and de Vries, 2010; Clark et al.,

62 2019) as a result of decreasing abundance of other species (Jung et al., 2018).
63 Additionally, soil Mn toxicity caused by soil acidification in calcareous grassland
64 asymmetrically curbed aboveground biomass of different species and functional groups
65 through suppression of photosynthesis (Tian et al., 2016).

66 A global meta-analysis with most data from forest ecosystems found negative
67 acidification effect on root biomass under sulfuric acid addition (Meng et al., 2019).
68 This was because forest soils with low initial pH ($\text{pH} < 5$) generally experienced greater
69 Al^{3+} and Fe^{3+} but less base cations, thus inhibiting root growth (Li et al., 2018).
70 Different from findings in forests, belowground biomass increased with soil
71 acidification in typical and alpine grasslands which was mainly due to the
72 compensatory growth concomitant with graminoids dominating over forbs (Chen et al.,
73 2015; Wang et al., 2020). Possibly, perennial rhizome grasses and sedges have higher
74 ionic tolerance (such as H^+ , Al^{3+} , NH_4^+ , and SO_4^{2-}) than perennial bunchgrasses and
75 forbs, which allowed for the maintenance of high community biomass under soil
76 acidification (Chen et al., 2015; Cliquet and Lemauviel-Lavenant, 2019; Wang et al.,
77 2020). Therefore, shifts in grassland community are mainly regulated by soil nutrient
78 fluctuations as induced by soil acidification that eventually affect above- and
79 belowground biomass (Mitchell et al., 2018; Wang et al., 2020).

80 Functional traits substantially influence plant survival, growth and reproduction via
81 closely associating with plant capability of resource acquisition (Violle et al., 2007).
82 Coping with environmental stresses to persist and reproduce, plants rely on a
83 combination of different functional traits ranging from conservative to acquisitive
84 strategies of resource acquisition (De Battisti et al., 2020). For example, some species
85 upregulate tissue nutrients as a fast resource acquisitive strategy when soil
86 environmental conditions become challenging (Mueller et al., 2012). On the opposite,
87 some plant species under environmental stresses tend to be more nutrient-conservative
88 by developing long-lasting leaves generally with a low specific leaf area (SLA) but a
89 high leaf dry matter content (LDMC) (Kandlikar et al., 2022). Grass species may also
90 increase root length to avoid acid and Al^{3+} stresses (Göransson et al., 2011). In general,
91 species with acquisitive strategy accumulate greater biomass in a rapid way, but species

92 with conservative strategy slow down biomass growth to elongate their life span (Reich,
93 2014; Hao et al., 2020).

94 Due to difficulties in measuring grassland root traits in situ, our understanding is
95 very limited in terms of using root trait strategy to explain the response of belowground
96 processes to soil acidification. Some plants can cope with nutrient deficiency in acidic
97 soils via modifications to their root morphologies and in their nutrient uptakes and
98 metabolisms (Hammond et al., 2004). Plants growing in resource-poor soils tend to
99 have lower specific root length (SRL) and lower root nutrient concentrations for the
100 conservation of resources (Delpiano et al., 2020). A pot experiment found that root
101 length of perennial grasses decreased with soil acidification, demonstrating the
102 constraint of root development in stressful circumstances (Haling et al., 2010). But in
103 natural ecosystems, grasses develop densely branched root systems with higher nutrient
104 use efficiency are more stress-tolerant to nutrient deficiency to maintain nutrient
105 balance and growth (Tian et al., 2022). Additionally, aboveground and belowground
106 biomass might also strongly and complicatedly be influenced by specific functional
107 traits (Clark et al., 2019; Wang et al., 2020), soil nutrient availability, and nutrient
108 contents and interactions in leaves and roots under soil acidification (Geng et al., 2014;
109 Rabêlo et al., 2018; Tian et al., 2021). Overall, it still remains elusive for how functional
110 traits in both above- and belowground components of different species respond to soil
111 acidification and their linkages with biomass.

112 To understand how soil acidification influences plant traits, biomass and their
113 relationships, we conducted a S addition experiment that included eight rates (from 0
114 to 50 g S m⁻² yr⁻¹) to simulate soil acidification in a semiarid grassland. We assessed the
115 role of plant above- and belowground traits and soil abiotic variables in driving the
116 grassland biomass of two dominate species (*Leymus chinensis* and *Carex duriuscula*)
117 under soil acidification. Specifically, we also aimed to quantify how these relationships
118 were modified by changes in soil conditions and related trait response strategy. The
119 perennial rhizome grass, a taller *L. chinensis* is widely distributed in arid and semi-arid
120 areas of northern China. This species occupies the top layers of the studied grassland
121 communities, likely giving it an advantage in resource acquisition, especially in terms

122 of light. Additionally, grasses generally exhibit flexibility in absorbing various soil N
123 forms, thereby expanding their ecological niche (Grassein et al., 2015). The perennial
124 rhizomatous sedge, a shorter subordinate species *C. duriuscula*, indicator plant for soil
125 degradation, possesses cluster root, tends to consume more photosynthetic products to
126 acquire nutrients (Zhang et al., 2021). Moreover, both species exhibit distinct
127 rhizosheaths that enable them to tightly adhere to the soil and show compensatory
128 growth in response to environmental disturbance (Tian et al., 2022). We addressed the
129 following questions: (i) how do soil properties (*i.e.* soil pH, Ca²⁺, Al³⁺, available N,
130 available P), above- and belowground plant traits (*i.e.* morphological and nutrient traits)
131 and biomass respond to different rates of S addition in the meadow grassland? (ii) What
132 are the key traits that correlate with the biomass responses of two species to soil
133 acidification? We hypothesize that soil acidification caused by S addition would lead to
134 a nutrient imbalance in grassland soil. Grass *L. chinensis* may respond to soil
135 acidification by adapting its aboveground light acquisition traits to maintain plant
136 biomass. However, in acidified soil, sedge *C. duriuscula* may employ the increased
137 tissue nutrient concentrations as a strategy to improve its acid resistance, which
138 subsequently leads to compensatory root growth (Fig. S1).

139 **2 Materials and methods**

140 **2.1 Experimental site and design**

141 This study was conducted at the Erguna Forest-Steppe Ecotone Research Station (50°
142 10' N, 119° 23' E) of Chinese Academy of Sciences in Inner Mongolia, China. The area
143 belongs to a transitional climate zone between mid-temperate to cold-temperate climate
144 with mean annual temperature and precipitation of -2.45 °C and 363 mm, respectively
145 (Feng et al., 2019). Soil in the experimental site is classified as a Haplic Chernozem
146 according to the Food and Agricultural Organization of the United Nations
147 classification and composed of 37 ± 0.9% sand, 40 ± 1.0% silt and 24 ± 0.8% clay.
148 Vegetation in this area is a meadow steppe community including common plant species
149 of *Leymus chinensis*, *Stipa baicalensis*, *Cleistogenes squarrosa*, *Carex duriuscula*,
150 *Pulsatilla turczaninovii*, and *Cymbaria dahurica*.

151 The experimental field was a natural steppe, which had been mown annually for
152 forage harvest until 2013, and fenced to exclude livestock grazing since then. A field
153 elemental S addition experiment was established in 2017 to simulate soil acidification
154 caused by atmospheric S deposition in a homogeneous and flat field containing
155 naturally assembled communities. The vegetation in the experimental plots is composed
156 of the dominant species (relative abundance >40 %) *Leymus chinensis*, subordinate
157 species (relative abundance between 1 % and 30 %), including *Stipa baicalensis*, *Carex*
158 *duriuscula*, *Cleistogenes squarrosa*, *Achnatherum sibiricum*, *Cymbaria dahurica*,
159 *Pulsatilla turczaninovii*, *Thermopsis lanceolala* and *Achnatherum sibiricum*. A
160 randomized block design was exploited included eight levels of S addition (0, 1, 2, 5,
161 10, 15, 20, and 50 g S m⁻² yr⁻¹), and each treatment had five replicates (Fig. S2). The
162 low dose S applications in our study was to imitate the current atmospheric SO₄²⁻
163 deposition level (2 - 4 g S m⁻² yr⁻¹) in the northeast of China (Yu et al., 2017). Each plot
164 (6 m × 6 m) was surrounded by 2-m wide buffer strips. Purified sulfur fertilizer
165 (elemental S > 99%) was mixed with 200 g soil collected from the untreated site nearby
166 and applied by hand spreading annually in late May since 2017. Sulfur powder in soil
167 can be oxidized by soil microorganisms to form H⁺ and SO₄²⁻ which can simulate soil
168 acidification well (Duddigan et al., 2021). In present study, we collected plant and soil
169 samples from 25 plots (five replicates) supplemented with five levels of S (0, 5, 10, 20,
170 and 50 g S m⁻²yr⁻¹).

171 2.2 Plant and soil sampling

172 In early August 2019, aboveground net primary productivity (ANPP) of plant
173 communities was collected from peak aboveground plant biomass because all
174 aboveground plant tissues would die during the winter. All living tissues were clipped
175 within a randomly selected 1 m × 1 m quadrat in each plot, sorted by species and oven-
176 dried at 65 °C for 48 h to measure peak species biomass and ANPP. The dried plant
177 samples were prepared to measure leaf nutrients.

178 We measured three aboveground morphological traits for two dominant species
179 *Leymus chinensis* (*L. chinensis*) and *Carex duriuscula* (*C. duriuscula*). Ten plant

180 individuals with complete shoot were randomly selected in each plot for each species.
181 These plant individuals were measured for maximum natural height and then clipped at
182 the ground level. All the samples immediately were placed in a portable refrigerator
183 and then detached to measure leaf area in laboratory. To guarantee water saturation of
184 the leaves, the sampled leaves were immersed in purified water and rehydrated for a
185 minimum period of 6 hours. Then the water-saturated leaves were carefully wiped off
186 the surface water with filter paper and weighed. The leaf area was scanned using a
187 scanner (Eption Perfection V39, Seiko Epson Corporation, Japan) and then dried at
188 60 °C for 72 h to weigh for dry mass. Specific leaf area (SLA, cm² g⁻¹) was calculated
189 as the ratio of leaf area to dry mass. Leaf dry matter content was calculated as the ratio
190 of dry mass to saturated mass (LDMC, g g⁻¹).

191 Plant roots were sampled using the soil block method in late August 2019.
192 Specifically, a 30 cm (length) × 30 cm (width) × 30 cm (depth) soil block was collected
193 using a steel plate and a shovel from each plot, resulting in a total of 25 soil blocks.
194 Each harvested soil block was immediately transported to the processing area and then
195 the soil blocks were gently loosened by hands to separate roots from soils. All separated
196 plant roots were carefully washed to remove the adhering soil and stored in iceboxes to
197 the laboratory. Before determining root morphological and chemical traits, all root
198 samples were frozen at -20 °C. At least 10 intact individual plants of *L. chinensis* and
199 *C. duriuscula* in each plot were used for determining root nutrient traits (root [N], [P],
200 [S], [Ca], [Fe], and [Mn]) and root morphological traits. Total root length, surface area
201 and volume were determined using the scanned images by the software of WinRHIZO
202 (Regent Instruments Inc., Quebec City, QC, Canada). Specific root length (SRL, m g⁻¹)
203 was calculated as total root length divided by its dry mass. Specific root surface area
204 (SRA, cm² g⁻¹) was defined as total surface area divided by its dry mass. Root tissue
205 density (RTD, g cm⁻³) was obtained as the ratio of root dry mass to its volume. All of
206 the above samples were dried at 65 °C to constant mass for determining root biomass
207 at species and community level. Root and leaf N concentrations were determined using
208 an elemental analyzer (Vario EL III, Elementar, Hanau, Germany). Both root and leaf
209 P, S, Ca, Fe and Mn concentrations were digested with 8 mL HNO₃ + 4 mL HClO₄ and

210 then determined by inductively coupled plasma optical emission spectrometry (5100
211 ICP-OES; Perkin Elmer, America).

212 **Fresh soil** sampling (0 - 10 cm depth) was performed using a soil auger (5 cm inner
213 diameter). For each plot, three cores were combined into one homogeneous sample.
214 After removing the visible plant detritus and rock, we sieved the fresh soils through a
215 2-mm screen and divided each soil sample into two subsamples. **Then a 10 g of fresh**
216 **soil** was immediately extracted with 2 mol L⁻¹ KCl solution. The extracted solution was
217 analyzed for nitrate (NO₃⁻) and ammonium (NH₄⁺) concentrations using an
218 autoAnalyser III continuous Flow Analyzer (Bran and Luebbe, Norderstedt, Germany).
219 The other subsample was air-dried for physicochemical properties determination. Soil
220 pH was determined in 2.5: 1 (v/w) water/soil ratio with a digital pH meter (Precision
221 and Scientific Instrument Co. Ltd., Shanghai, China). Soil available P concentration
222 was extracted with 0.5 mol L⁻¹ NaHCO₃ solution and soil available S concentration was
223 extracted with 0.1 mol L⁻¹ Ca(H₂PO₄)₂ (Tabatabai and Bremner, 1972) following
224 absorbance measurement on a UV-VIS spectrophotometer (UV-1700, Shimadzu, Japan)
225 at 880 nm and 440 nm, respectively. **Soil exchangeable aluminum (Al³⁺) concentration**
226 **was measured using titration by 0.25 M NaOH to pH 7.0 after extraction with 1 M KCl**
227 **solution from air-dried soil samples. Soil exchangeable calcium (Ca²⁺) was extracted**
228 **by 1 M NH₄OAc (pH = 7.0) at a 1:10 ratio (w/v) for 30 min. Diethylene triamine**
229 **pentaacetic acid (DTPA)-Fe and Mn were extracted from 10 g of air-dried soil sample**
230 **with 20 ml of 0.005 M diethylenetriamine pentaacetic acid (DTPA), 0.01 M CaCl₂, and**
231 **0.1 M triethanolamine (TEA) at pH 7.3 and determined using an atomic absorption**
232 **spectrophotometer (AAS, Shimadzu, Japan) (Feng et al., 2019; Li et al., 2021).**

233 **2.3 Statistical analyses**

234 The effects of S addition on soil properties, plant traits and biomass were analyzed using
235 one-way analysis of variance (ANOVA) with Duncan test. Pearson's correlation
236 analysis was used to explore the relationship between plant traits, plant biomass and
237 soil abiotic variables across the S-addition levels. All these statistical analyses were
238 performed using SPSS16.0 (SPSS Inc., Chicago, USA) with significance accepted at *p*

239 < 0.05.

240 We used structural equation modelling (SEM) to analyze the indirect effects of S
241 addition meditating grassland plant aboveground and root biomass from the perspective
242 of plant traits and soil factors. Prior to SEM analysis, the number of variables were
243 reduced by conducting principal component analysis (PCA) on soil variables (pH,
244 $\text{NH}_4^+\text{-N}$, $\text{NO}_3^-\text{-N}$, available P, available S, exchangeable cations Ca^{2+} and Al^{3+} , DTPA-
245 Fe and DTPA-Mn), aboveground morphological traits (Height, SLA, LDMC), leaf
246 nutrient traits (Ca, Fe, Mn), root morphological traits (SRL, SRA, RTD) and root
247 nutrient traits (N, P, S, Ca, Fe, Mn) of the two species. We then used the first principal
248 components (PC1) for the subsequent SEM analysis to represent soil acidification (PC1
249 explained 94.8% of the variation), soil nutrients (PC1 explained 62.3% of the variation),
250 root nutrient traits in *C. duriuscula* (PC1 explained 45.7% of the variation),
251 aboveground morphological traits in *L. chinensis* (PC1 explained 54.7% of the variation)
252 (Table S1). A conceptual model of hypothetical relationships was constructed (Fig. S1),
253 assuming that S addition would directly impact [soil physicochemical properties, and](#)
254 [indirectly influence](#) aboveground and belowground biomass through altering soil pH,
255 soil nutrient availability and plant traits. The SEM analyses were performed using
256 [AMOS 24.0 \(Amos Development Co., Maine, USA\)](#) and the PCA analyses were
257 performed using the vegan package in R 4.2.2.

258

259 **3 Results**

260 **3.1 Effects of S addition on soil properties**

261 Sulfur addition significantly decreased soil pH from 6.95 to 5.19, but increased soil
262 exchangeable Al concentration only in the highest S-addition level of $50 \text{ g S m}^{-2} \text{ yr}^{-1}$
263 (Table 1). Similarly, S addition increased soil ammonium concentration but decreased
264 nitrate concentration in the highest S addition treatment compared to the control (Table
265 1). Soil available P, available S, DTPA-Fe and DTPA-Mn concentration increased with
266 increasing S addition rate, while soil exchangeable Ca concentration decreased (Table
267 1).

268 **3.2 Effects of S addition on above- and belowground biomass**

269 In the third year, S addition suppressed aboveground biomass of plant community (Fig.
270 1). Aboveground biomass of the two dominant species showed contrasting responses to
271 S addition, with an increase for *C. duriuscula* but a decrease for *L. chinensis* (Fig. 1).
272 Moreover, S addition significantly increased belowground biomass of plant community
273 owing to the increase in *C. duriuscula*, while it had no impact on the belowground
274 biomass of *L. chinensis* (Fig. 1).

275 **3.3 Effects of S addition on above- and belowground traits of *L.*** 276 ***chinensis* and *C. duriuscula***

277 For the morphological traits, S addition enhanced plant height of *C. duriuscula*, but had
278 no impact on *L. chinensis* (Fig. 2a). Sulfur addition significantly decreased SLA and
279 increased LDMC of *L. chinensis*, whereas it had no effect on that of *C. duriuscula* (Fig.
280 2b and c). For the belowground tissues, S treatment increased SRL in two species, and
281 only decreased SRA of *C. duriuscula* (Fig. 2d and e). However, RTD showed no
282 significant change for the two species (Fig. 2f).

283 For the nutrient traits, S addition had no impact on leaf [N], [P], and [Ca], and
284 increased leaf [S] and [Mn] of the two species, while decreased leaf [Fe] of *C.*
285 *duriuscula* but increased leaf [Fe] of *L. chinensis* (Fig. 3). An increase in root [N], root
286 [P], root [S] of *C. duriuscula* was found under S addition, but not for *L. chinensis* (Fig.
287 3h, i and j). Sulfur addition decreased root [Ca] of *C. duriuscula*, but had no impact on
288 *L. chinensis* (Fig. 3k). Root [Fe] showed similar patterns with leaf [Fe] with a decrease
289 in *C. duriuscula* and an increase in *L. chinensis* (Fig. 3l). Root [Mn] of species were
290 enhanced by S addition (Fig. 3m).

291 **3.4 Correlations and pathways of S-induced soil acidification effects** 292 **on plant traits and biomass**

293 According to correlation analysis (Figs. S3 and S4), the aboveground morphological
294 traits, leaf and the root nutrient traits showed species-specific responses. This was
295 mainly due to the increase in soil acidity, Al³⁺ toxicity and nutrient imbalance (*i.e.*, the

296 deficient or excessive of certain nutrients in the soil) induced by S addition, which fitted
297 the structural equation modelling (SEM) well ($\chi^2 = 51.83$, $P = 0.10$, $df = 40$, $AIC =$
298 103.83 , $n = 25$) (Fig. 4). The indirect positive effect of S addition on community
299 belowground biomass was mainly implemented through decreasing soil pH together
300 with the imbalance of soil available nutrients, altering the leaf and root nutrient traits,
301 and the belowground biomass and of *C. duriuscula*, which accounted for 69% of the
302 variation in community belowground biomass (Fig. 4). The indirect negative effect of
303 S addition on community aboveground biomass was mainly achieved through soil
304 acidification, the aboveground morphological traits and aboveground biomass of *L.*
305 *chinensis*, which accounted for 59% of the variation in community aboveground
306 biomass (Fig. 4).

307 **4. Discussion**

308 **4.1 Species-specific trait responses to S addition**

309 Trait response patterns was different between *L. chinensis* and *C. duriuscula* under S
310 addition. Specifically, nutrient traits of *L. chinensis* were less plastic, as evidenced by
311 unchanged concentrations of N, P, S, and Ca, comparing with *C. duriuscula*. Indeed, *L.*
312 *chinensis* was suggested to be a highly homeostatic species with greater stability in
313 elemental composition in a temperate steppe (Yu et al., 2010). Higher macroelement
314 homeostasis helps plant maintain function and productivity stability to resist changes
315 in soil environment (Yu et al., 2010; Feng et al., 2019).

316 It was interesting to note that both leaf and root [Fe] in *L. chinensis* increased with
317 S addition and were not associated with soil available [Fe] (Figs. 3 and S3). Iron uptake
318 and assimilation had been shown to be dependent on sulfate availability (Zuchi et al.,
319 2012). Previous research demonstrated close relationships between Fe and S nutrition,
320 suggesting common regulatory mechanisms for the homeostasis of the two elements
321 (Forieri et al., 2013). For grasses, S addition could enhance assimilation of plant S and
322 subsequently incorporated into methionine in order to accelerate the secretion of
323 phytosiderophore (Zuchi et al., 2012; Courbet et al., 2019). However, Fe absorption of
324 *C. duriuscula* was inhibited by soil acidification which was consistent with Fe (III)-

325 reduction-based mechanism (Tian et al., 2016). Namely, acquisition of Fe by non-
326 graminaceous monocotyledonous species was mediated by the reduction of Fe^{3+} to Fe^{2+}
327 catalyzed by the ferric chelate reductase in root cells, and Fe^{2+} absorption can be further
328 curbed by the competition with Mn^{2+} for the same metal transporter (Curie and Briat,
329 2003; Pittman, 2005). Acidification-induced higher soil DTPA-Mn concentration in the
330 calcareous soil contributed to Mn accumulation in plant tissues of the two species (Figs.
331 3 and 5). Sulfur addition increased tissue [Mn] greater in *C. duriuscula* than in *L.*
332 *chinensis*.

333 *L. chinensis* decreased SLA and increased LDMC to reduce the loss of water and
334 nutrients, which showed conservative resource-uptake strategy under soil acidification
335 stress. The variations in SLA and LDMC of *L. chinensis* were significantly correlated
336 with soil exchangeable Al, implying that conservative traits might also link with Al-
337 resistant strategy of species (Poozesh et al., 2007). As soil pH decreased, soil nitrate
338 was reduced and positively correlated with SLA but negatively with LDMC of *L.*
339 *chinensis* (Table 1 and Fig. S3). Soil nitrification had been shown to be positively
340 related to leaf traits (such as leaf [N] and SLA) (Laughlin et al., 2011). This suggested
341 that the decrease of soil nitrate under soil acidification could be an important driver of
342 plant trait variation. For *L. chinensis*, belowground traits were insensitive to S addition
343 as compared with *C. duriuscula*. One possible explanation for this insensitivity might
344 be that deep-rooted species were much more resistant to changing soil environment
345 than the shallow-rooted species (such as sedge *C. duriuscula*) (Zhang et al., 2019). We
346 found both species invested more in enhancing SRL under soil acidification, which was
347 in agreement with Göransson et al. (2011) that grass species increased root length to
348 avoid acid stress. These results indicated that variation of root morphological traits has
349 the potential to mitigate the negative effects of soil acidity and should be considered as
350 part of stress-avoidance or tolerance strategies (Thomaes et al., 2013).

351 **4.2 Species-specific and community biomass responses to S addition**

352 To clarify the underlying mechanisms, we explored the important role of morphological
353 and nutrient traits in mediating aboveground and belowground biomass changes under

354 S addition. We found that aboveground and root traits of two species exhibited
355 contrasting adaptive strategies in acquiring aboveground and belowground resources
356 which were associated with their biomass (Figs. 4 and 5). Importantly, SEM showed
357 that the decrease in aboveground biomass of *L. chinensis* was related to the increased
358 soil acidification and the conservative responses in aboveground morphological traits
359 under S addition (Figs. 4 and 5). *L. chinensis* seemed to be a nitrophilic and resource-
360 acquisitive species under N-rich environment (Feng et al., 2019; Yang et al., 2019), but
361 it was at a disadvantage under S-induced soil acidification. For example, we found SLA
362 and LDMC in *L. chinensis* were positively correlated with the aboveground biomass of
363 both *L. chinensis* and plant community (Fig. S3). Soil acidification resulted in enhanced
364 toxic effects of proton and exchangeable Al (Roem and Berndse, 2000). From
365 environmental stress hypothesis perspective, the species could employ different
366 strategies to mitigate such environmental stress which associated with trait responses
367 (Encinas-Valero et al., 2022). Usually, SLA and LDMC were prominent indicators of
368 plant strategy with respect to productivity as related to environmental stress and
369 disturbance regimes. Stress tolerant species normally had lower growth rates,
370 photosynthetic rates, and SLA but higher LDMC (Pérez-Harguindeguy et al., 2013).
371 Sulfur addition induced acidity stress for plants, leading to reduced SLA accompanied
372 with lower photosynthesis and decreased plant aboveground productivity. Damages in
373 photosynthetic function accompanied by oxidative stress were found in woody tree
374 species under the threat of acid rain (Chen et al., 2013b), it is still less understanding to
375 physiological and biochemical responses of different functional groups to soil
376 acidification in grassland ecosystems. The future researches about plant photosynthetic
377 and antioxidant responses by soil acidification are critically needed to test.

378 We found that plant community aboveground biomass exhibited a tendency to
379 decline from 22% to 11% under soil acidification, although the overall effect was rather
380 weak between pH 6.7 and pH 5.19 (Fig. 1, Table 1). Notably, *L. chinensis* played a
381 dominant role in aboveground productivity which was consistent with the finding that
382 grasses occupied a mean coverage of around 60% in acid grassland and Heathland
383 (Tibbett et al., 2019). Therefore, the decreasing aboveground biomass of *L. chinensis*

384 was one reason for the decline of community aboveground productivity (Fig. 4).
385 Another explanation for the decline of aboveground biomass may be competitive
386 exclusion of bunchgrasses and forbs under soil acidification (Stevens et al., 2010; Chen
387 et al., 2015). Together, our study contributes to a deeper understanding that leaf
388 morphological traits of dominant species play a crucial role in regulating grassland
389 productivity in response to soil acidification.

390 In contrast, belowground biomass of *C. duriuscula* and plant community both
391 significantly increased (ranging from 19 to 52%) with soil acidification (Fig. 1). Sedge
392 (*C. duriuscula*) was more tolerant than perennial rhizome grass (*L. chinensis*) under
393 soil acidification. This was partly supported by similar results obtained in alpine and
394 typical steppe grassland ecosystems (Chen et al., 2015; Wang et al., 2020). Previous
395 studies suggested that the sedge had a greater competitive advantage in nutrient-poor
396 environments than other functional groups (Gusewell, 2004). An increase in root
397 biomass under soil acidification suggested that sedge invested more resources in
398 nutrient acquisition. SEM provided further evidence that for *C. duriuscula*, the higher
399 nutrient demand (such as root [N], [P], [S], [Mn]) was matched by high root biomass
400 investment under S treatment (Fig. 4). The increased root biomass of *C. duriuscula*
401 promoted the increased belowground biomass of plant community which could be
402 related to the shifts in soil available nutrients under S addition. Our present study
403 provided direct evidence that *C. duriuscula* was considered to be a high nutrient-
404 requiring species and thereby its biomass growth increased with soil acidification stress
405 (Figs. 4 and 5). Our short-term findings suggest that the sedge play an important role in
406 preventing the decline of grassland productivity in acidified soils, reflecting transient
407 dynamics. Consistent with results from a long-term acidification experiment (Tibbett et
408 al., 2019), compensatory growth of acid-tolerant species is probably key to maintain
409 grassland productivity over the long term, particularly for ecosystems that experience
410 acidification by chronic N and S deposition.

411 For grassland ecosystems, most of the carbon is allocated belowground (Bontti et
412 al., 2009). Accumulation of roots may benefit competition for nutrient and water
413 resources in a short-term (Wang et al., 2020). In the long-term, however, asymmetric

414 light competitive advantage of larger individuals (*L. chinensis*) rather than the
415 competition of soil resources (DeMalach and Kadmon, 2017), will make a decisive
416 effect on community productivity and diversity under soil acidification. Contrary to
417 previous findings by Wang et al. (2020), who reported that diameter of 3rd-order roots
418 contributed to the increase of community belowground biomass under soil acidification
419 in an alpine grassland. Our study provided a novel insight that leaf and root nutrients
420 as a whole jointly mediated community belowground biomass with soil acidification
421 induced by S addition.

422 **5 Conclusion**

423 Our results highlighted that aboveground and root traits played important roles in
424 mediating grassland plant competition for environment resources under soil
425 acidification. Sulfur addition acidified soils, and lead to nutrient imbalance (higher
426 ammonium, available P, Fe, Mn and exchangeable Al³⁺, but lower nitrate and
427 exchangeable Ca²⁺). The **dominant** species *L. chinensis* showed conservative strategy,
428 with decreased SLA and increased LDMC in response to S addition. Moreover,
429 conservative traits were linked with stable root biomass but lower aboveground
430 biomass as a direct impact from soil acidification. Conversely, *C. duriuscula* displayed
431 acquisitive strategy, with increased shoot height and root traits ([N], [P], [S], [Mn],
432 SRL) promoting both aboveground and root biomass under S addition, as mediated via
433 altered soil acidity and nutrient availability. Such divergent and species-specific
434 responses was strongly driven by soil environmental conditions which resulted in
435 inconsistent responses of grassland community aboveground and belowground biomass
436 to S addition. As continuous S deposition causes widespread acidification and soil
437 functional degradation problems across the world, our results implied the important
438 roles of both aboveground and root traits in regulating species and community biomass
439 under soil acidification.

440

441 *Author contributions.* All authors contributed to the design of the study. TL and HL
442 conducted the experimental work and the data analysis. XF wrote the manuscript with

443 RW, JC and YJ.

444

445 *Competing interests.* None of the authors have a conflict of interest.

446

447 *Acknowledgements.* We would like to acknowledge the support from Youth
448 Innovation Promotion Association of Chinese Academy of Sciences.

449

450 *Financial support.* This research was supported by the National Natural Science
451 Foundation of China (32271677, 32071563, 32222056 and 32271655), the Strategic
452 Priority Research Program of the Chinese Academy of Sciences (XDA23080400), and
453 the Doctoral Science Foundation of Liaoning Province (2021-BS-015).

454

455

456 *Data availability.* Data will be made available on request from the corresponding
457 author.

458

459 **References**

460 Bolan, N. S., Adriano, D. C., and Curtin, D.: Soil acidification and liming interactions
461 with nutrient and heavy metal transformation and bioavailability, *Adv. Agron.*,
462 78, 5-272, [https://doi.org/10.1016/S0065-2113\(02\)78006-1](https://doi.org/10.1016/S0065-2113(02)78006-1), 2003.

463 Bontti, E. E., Decant, J. P., Munson, S. M., Gathany, M. A., Przeszlowska, A., Haddix,
464 M. L., Owens, S., Burke, I. C., Parton, W. J., and Harmon, M. E.: Litter
465 decomposition in grasslands of central North America (US Great Plains), *Global*
466 *Chang Biol.*, 15, 1356-1363. <https://doi.org/10.1111/j.1365-2486.2008.01815.x>,
467 2009.

468 Chen, D., Lan, Z., Bai, X., Grace, J. B., and Bai, Y.: Evidence that acidification-
469 induced declines in plant diversity and productivity are mediated by changes in
470 below-ground communities and soil properties in a semi-arid steppe, *J. Ecol.*,

471 101, 1322-1334, <https://doi.org/10.1111/1365-2745.12119>, 2013a.

472 Chen, D., Wang, Y., Lan, Z., Li, J., Xing, W., Hu, S. and Bai, Y.: Biotic community
473 shifts explain the contrasting responses of microbial and root respiration to
474 experimental soil acidification, , 90, 139-147,
475 <https://doi.org/10.1016/j.soilbio.2015.08.009>, 2015.

476 Chen, J., Wang, W. H., Liu, T., Wu, F., and Zheng, H.: Photosynthetic and antioxidant
477 responses of *Liquidambar formosana* and *Schima superba* seedlings to sulfuric-
478 rich and nitric-rich simulated acid rain. *Plant Physiol. Bioch.*, 64, 41-51,
479 <https://doi.org/10.1016/j.plaphy.2012.12.012>, 2013b.

480 Clark, C. M., Simkin, S. M., Allen, E. B., Bowman, W. D., Belnap, J., Brooks, M. L.,
481 Collins, S. L., Geiser, L. H., Gilliam, F. S., Jovan, F. S., Pardo, L. H., Schulz, B.
482 K., Stevens, C. J., Suding, K. N., Throop, H. L., and Waller, D. M.: Potential
483 vulnerability of 348 herbaceous species to atmospheric deposition of nitrogen
484 and sulfur in the United States, *Nat. Plants*, 5, 697-705, <https://doi.org/10.1038/s41477-019-0442-8>, 2019.

486 Cliquet, J. B. and Lemauiel-Lavenant, S.: Grassland species are more efficient in
487 acquisition of S from the atmosphere when pedospheric S availability decreases,
488 *Plant Soil*, 435, 69-80, <https://doi.org/10.1007/s11104-018-3872-6>, 2019.

489 Courbet, G., Gallardo, K., Vigani, G., Brunel-Muguet, S., Trouverie, J., Salon, C., and
490 Ourry, A.: Disentangling the complexity and diversity of crosstalk between sulfur
491 and other mineral nutrients in cultivated plants, *J. Exp. Bot.*, 70, 4183-4196,
492 <https://doi.org/10.1093/jxb/erz214>, 2019.

493 Curie, C. and Briat, J. F.: Iron transport and signaling in plants, *Annu. Rev. Plant*
494 *Biol.*, 54, 183-206, <https://doi.org/10.1146/annurev.arplant.54.031902.135018>,
495 2003.

496 De Battisti, D., Fowler, M. S., Jenkins, S. R., Skov, M. W., Bouma, T. J., Neyland, P.
497 J., and Griffin, J. N.: Multiple trait dimensions mediate stress gradient effects on
498 plant biomass allocation, with implications for coastal ecosystem services, *J.*
499 *Ecol.*, 108, 1227-1240, <https://doi.org/10.1111/1365-2745.13393>, 2020.

500 Delpiano, C.A., Prieto, I., Loayza, A.P., Carvajal, D.E., and Squeo, F.A.: Different

501 [responses of leaf and root traits to changes in soil nutrient availability do not](#)
502 [converge into a community-level plant economics spectrum. Plant Soil 450, 463-](#)
503 [478, <https://doi.org/10.1007/s11104-020-04515-2>, 2020.](#)

504 DeMalach, N. and Kadmon, R.: Light competition explains diversity decline better
505 than niche dimensionality, *Funct. Ecol.*, 31, 1834-1838, [https://doi.org/10.1111/](https://doi.org/10.1111/1365-2435.12841)
506 [1365-2435.12841](https://doi.org/10.1111/1365-2435.12841), 2017.

507 Duan, L., Yu, Q., Zhang, Q., Wang, Z., Pan, Y., Larssen, T., Tang, J., and Mulder, J.:
508 Acid deposition in Asia: Emissions, deposition, and ecosystem effects,
509 *Atmospheric Environ.*, 146, 55-69, [http://doi.org/10.1016/j.atmosenv.2016.07.](http://doi.org/10.1016/j.atmosenv.2016.07.018)
510 [018](http://doi.org/10.1016/j.atmosenv.2016.07.018), 2016.

511 Duddigan, S., Fraser, T., Green, I., Diaz, A., Sizmur, T., and Tibbett, M.: Plant, soil
512 and faunal responses to a contrived pH gradient, *Plant Soil*, 462, 505-524,
513 <https://doi.org/10.1007/s11104-021-04879-z>, 2021.

514 Encinas-Valero, M., Esteban, R., Hereş, A. M., Vivas, M., Fakhet, D., Aranjuelo, I.,
515 Solla, A., Moreno, G., and Curiel Yuste, J.: Holm oak decline is determined by
516 shifts in fine root phenotypic plasticity in response to belowground stress, *New*
517 *Phytol.*, 235, 2237-2251, <https://doi.org/10.1111/nph.18182>, 2022.

518 Feng, X., Wang, R., Yu, Q., Cao, Y., Zhang, Y., Yang, L., Dijkstra, F. A., and Jiang, Y.:
519 Decoupling of plant and soil metal nutrients as affected by nitrogen addition in a
520 meadow steppe, *Plant Soil*, 443, 337-351, [https://doi.org/10.1007/s11104-019 -](https://doi.org/10.1007/s11104-019-04217-4)
521 [04217-4](https://doi.org/10.1007/s11104-019-04217-4), 2019.

522 Forieri, I., Wirtz, M., and Hell, R.: Toward new perspectives on the interaction of iron
523 and sulfur metabolism in plants, *Front. Plant Sci.*, 4, 357, [https://doi.org/10.3389](https://doi.org/10.3389/fpls.2013.00357)
524 [/fpls.2013.00357](https://doi.org/10.3389/fpls.2013.00357), 2013.

525 Garrison, M. T., Moore, J. A., Shaw, T. M., and Mika, P. G.: Foliar nutrient and tree
526 growth response of mixed-conifer stands to three fertilization treatments in
527 northeast Oregon and north central Washington, *For. Ecol. Manag.*, 132, 183-
528 198, [https://doi.org/10.1016/S0378-1127\(99\)00228-5](https://doi.org/10.1016/S0378-1127(99)00228-5), 2000.

529 Geng, Y., Wang, L., Jin, D., Liu, H., and He, J.: Alpine climate alters the relationships
530 between leaf and root morphological traits but not chemical traits, *Oecologia*,

531 175, 445-455, <https://doi.org/10.1007/s00442-014-2919-5>, 2014.

532 Göransson, P., Falkengren-Grerup, U., and Andersson, S.: *Deschampsia cespitosa* and
533 soil acidification: general and trait-specific responses to acid and aluminium
534 stress in a solution experiment, *Nord. J. Bot.*, 29, 97-104, [https://doi.org/10.1111](https://doi.org/10.1111/j.1756-1051.2010.00793.x)
535 [/j.1756-1051.2010.00793.x](https://doi.org/10.1111/j.1756-1051.2010.00793.x), 2011.

536 Grassein, F., Lemauiel- Lavenant, S., Lavorel, S., Bahn, M., Bardgett, R. D.,
537 Desclos- Theveniau, M., and Lâiné, P.: Relationships between functional traits
538 and inorganic nitrogen acquisition among eight contrasting European grass
539 species. *Ann. Bot.*, 115, 107-115, <https://doi.org/10.1093/aob/mcu233>, 2015.

540 Gusewell, S.: N: P ratios in terrestrial plants: Variation and functional significance.
541 *New Phytol.*, 164, 243-266, <https://doi.org/10.1111/j.1469-8137.2004.01192.x>,
542 2004.

543 Haling, R. E., Richardson, A. E., Culvenor, R. A., Lambers, H., and Simpson, R. J.:
544 Root morphology, root-hair development and rhizosheath formation on perennial
545 grass seedlings is influenced by soil acidity, *Plant Soil*, 335, 457-468, [https://](https://doi.org/10.1007/s11104-010-0433-z)
546 doi.org/10.1007/s11104-010-0433-z, 2010.

547 Hammond, J.P., Broadley, M. R., and White, P. J.: Genetic responses to phosphorus
548 deficiency. *Ann. Bot.*, 94, 323-332, <https://doi.org/10.1093/aob/mch156>, 2004.

549 Hao, M., Messier, C., Geng, Y., Zhang, C., Zhao, X., and von Gadow, K.: Functional
550 traits influence biomass and productivity through multiple mechanisms in a
551 temperate secondary forest, *Eur. J. For. Res.*, 139, 959-968, [https://doi.org/10.](https://doi.org/10.1007/s10342-020-01298-0)
552 [1007/s10342-020-01298-0](https://doi.org/10.1007/s10342-020-01298-0), 2020.

553 Jaggi, R. C., Aulakh, M. S., and Sharma, R.: Impacts of elemental S applied under
554 various temperature and moisture regimes on pH and available P in acidic,
555 neutral and alkaline soils, *Biol. Fert. Soils*, 41, 52-58,
556 <https://doi.org/10.1007/s00374-004-0792-9>, 2005.

557 Jung, K., Kwak, J. H, Gilliam, F. S., and Chang, S. X.: Simulated N and S deposition
558 affected soil chemistry and understory plant communities in a boreal forest in
559 western Canada. *J. Plant Ecol.*, 11, 511-523, <https://doi.org/10.1093/jpe/rtx030>,
560 2018.

561 Kandlikar, G. S., Kleinhesselink, A. R., and Kraft, N. J.: Functional traits predict
562 species responses to environmental variation in a California grassland annual
563 plant community, *J. Ecol.*, 110, 833-844, [https://doi.org/10.1111/1365-](https://doi.org/10.1111/1365-2745.13845)
564 2745.13845, 2022.

565 Kemmitt, S. J., Wright, D., and Jones, D. L.: Soil acidification used as a management
566 strategy to reduce nitrate losses from agricultural land, *Soil Biol. Biochem.*, 37,
567 867-875, <https://doi.org/10.1016/j.soilbio.2004.10.001>, 2005.

568 Laughlin, D.C.: Nitrification is linked to dominant leaf traits rather than functional
569 diversity, *J. Ecol.*, 99, 1091-1099, [https://doi.org/10.1111/j.1365-2745.2011.](https://doi.org/10.1111/j.1365-2745.2011.01856.x)
570 01856.x, 2011.

571 Leifeld, J., Bassin, S., Conen, F., Hajdas, I., Egli, M., and Fuhrer, J.: Control of soil
572 pH on turnover of belowground organic matter in subalpine grassland,
573 *Biogeochemistry*, 112, 59-69, <https://doi.org/10.1007/s10533-011-9689-5>, 2013.

574 Li, T., Wang, R., Cai, J., Meng, Y., Wang, Z., Feng, X., Liu, H., Turco, R. F., and
575 Jiang, Y.: Enhanced carbon acquisition and use efficiency alleviate microbial
576 carbon relative to nitrogen limitation under soil acidification, *Ecol. Process*, 10,
577 1-13, <https://doi.org/10.1186/s13717-021-00309-1>, 2021.

578 Li, Y., Sun, J., Tian, D., Wang, J., Ha, D., Qu, Y., Jing, G., and Niu, S.: Soil acid
579 cations induced reduction in soil respiration under nitrogen enrichment and soil
580 acidification, *Sci. Total Environ.*, 615, 1535-1546, [http://doi.org/10.1016/j.](http://doi.org/10.1016/j.scitotenv.2017.09.131)
581 scitotenv.2017.09.131, 2018.

582 Meng, C., Tian, D., Zeng, H., Li, Z., Yi, C., and Niu, S.: Global soil acidification
583 impacts on belowground processes, *Environ. Res. Lett.*, 14, 074003, [https://](https://doi.org/10.1088/1748-9326/ab239c)
584 doi.org/10.1088/1748-9326/ab239c, 2019.

585 Mitchell, R. J., Hewison, R. L., Fielding, D. A., Fisher, J. M., Gilbert, D. J.,
586 Hurskainen, S., Pakeman, R.J., Potts, J. M., and Riach, D.: Decline in
587 atmospheric sulphur deposition and changes in climate are the major drivers of
588 long-term change in grassland plant communities in Scotland, *Environ. Pollut.*,
589 235, 956-964, [https:// doi.org/10.1016/j.envpol.2017.12.086](https://doi.org/10.1016/j.envpol.2017.12.086), 2018.

590 Mueller, K. E., Eissenstat, D. M., Hobbie, S. E., Oleksyn, J., Jagodzinski, A. M.,

591 Reich, P. B., Chadwick, O. A., and Chorover, J.: Tree species effects on coupled
592 cycles of carbon, nitrogen, and acidity in mineral soils at a common garden
593 experiment, *Biogeochemistry*, 111, 601-614, <https://doi.org/10.1007/s10533-011->
594 9695-7, 2012.

595 Pérez-Harguindeguy, N., Diaz, S., Garnier, E., Lavorel, S., Poorter, H., Jaureguiberry,
596 P., Bret-Harte, M. S., Cornwell, W. K., Craine, J. M., Gurvich, D. E., Urcelay, C.,
597 Veneklaas, E. J., Reich, P. B., Poorter, L., Wright, I. J., Ray, P., Enrico, L.,
598 Pausas, J. G., de Vos, A. C., Buchmann, N., Funes, G., Quetier, F., Hodgson, J.
599 G., Thompson, K., Morgan, H. D., ter Steege, H., van der Heijden, M. G. A.,
600 Sack, L., Blonder, B., Poschlod, P., Vaieretti, M. V., Conti, G., Staver, A. C.,
601 Aquino, S., and Cornelissen, J. H. C.: New handbook for standardised
602 measurement of plant functional traits worldwide, *Aust. Bot.*, 61, 167-234,
603 <http://doi.org/10.1071/BT 12225>, 2013.

604 Pittman, J. K.: Managing the manganese: molecular mechanisms of manganese
605 transport and homeostasis, *New Phytol.*, 167, 733-742, <http://doi.org/10.1111/>
606 [j.1469-8137.2005.01453.x](http://doi.org/10.1111/j.1469-8137.2005.01453.x), 2005.

607 Poozesh, V., Cruz, P., Choler, P., and Bertoni, G., Relationship between the Al
608 resistance of grasses and their adaptation to an infertile habitat, *Ann. Bot.*, 99,
609 947-954, <https://doi.org/10.1093/aob/mcm046>, 2007.

610 Rabêlo, F. H. S., Lux, A., Rossi, M. L., Martinelli, A. P., Cuypers, A., and Lavres, J.
611 Adequate S supply reduces the damage of high Cd exposure in roots and
612 increases N, S and Mn uptake by Massai grass grown in hydroponics, *Environ.*
613 *Exp. Bot.*, 148, 35-46, <https://doi.org/10.1016/j.envexpbot.2018.01.005>, 2018.

614 Reich, P. B.: The world-wide ‘fast-slow’ plant economics spectrum: a traits manifesto,
615 *J. Ecol.*, 102, 275-301, <https://doi.org/10.1111/1365-2745.12211>, 2014.

616 Roem, W. J. and Berendse, F.: Soil acidity and nutrient supply ratio as possible factors
617 determining changes in plant species diversity in grassland and heathland
618 communities, *Biol. Conserv.*, 92, 151-161, <https://doi.org/10.1016/S0006-3207>
619 (99)00049-X, 2000.

620 Stevens, C. J., Thompson, K., Grime, J. P., Long, C. J., and Gowing, D. J.:

621 Contribution of acidification and eutrophication to declines in species richness of
622 calcifuge grasslands along a gradient of atmospheric nitrogen deposition, *Funct.*
623 *Ecol.*, 24, 478-484, <https://doi.org/10.1111/j.1365-2435.2009.01663.x>, 2010.

624 Thomaes, A., De Keersmaecker, L., De Schrijver, A., Baeten, L., Vandekerckhove, K.,
625 Verstraeten, G., and Verheyen, K.: Can soil acidity and light help to explain tree
626 species effects on forest herb layer performance in post-agricultural forests?,
627 *Plant Soil*, 373, 183-199, <https://doi.org/10.1007/s11104-013-1786-x>, 2013.

628 Tian, D. and Niu, S.: A global analysis of soil acidification caused by nitrogen
629 addition, *Environ. Res. Lett.*, 10, 024019, [https://doi.org/10.1088/1748-](https://doi.org/10.1088/1748-9326/10/2/024019)
630 [9326/10/2/024019](https://doi.org/10.1088/1748-9326/10/2/024019), 2015.

631 Tian, Q., Liu, N., Bai, W., Li, L., Chen, J., Reich, P. B., Yu Q., Guo, D., Smith, M. D.,
632 Knapp, A. K., Cheng, W., Lu, P., Gao, Y., Yang, A., Wang, T., Li, X., Wang, Z.,
633 Ma, Y., and Zhang, W.: A novel soil manganese mechanism drives plant species
634 loss with increased nitrogen deposition in a temperate steppe, *Ecology*, 97, 65-
635 74, <https://doi.org/10.1890/15-0917.1>, 2016.

636 Tian, Q., Lu, P., Ma, P., Zhou, H., Yang, M., Zhai, X. Chen M., Wang, H., Li W., Bai,
637 W., Lambers, H., and Zhang, W.: Processes at the soil-root interface determine
638 the different responses of nutrient limitation and metal toxicity in forbs and
639 grasses to nitrogen enrichment, *J. Ecol.*, 109, 927-938,
640 <https://doi.org/10.1111/1365-2745.13519>, 2021.

641 [Tian, Q., Lu, P., Zhai, X., Zhang, R., Zheng, Y., Wang, H., Nie, B., Bai, W., Niu, S.,](#)
642 [Shi, P., Yang, Y., Yang, D., Stevens, C., Lambers, H., and Zhang, W.: An](#)
643 [integrated belowground trait - based understanding of nitrogen - driven plant](#)
644 [diversity loss. *Global Change Biol.*, 28, 3651-3664, \[https://doi.org/10.1111/\]\(https://doi.org/10.1111/gcb.16147\)](#)
645 [gcb.16147](#), 2022.

646 Tibbett, M., Gil-Martínez, M., Fraser, T., Green, I. D., Duddigan, S., De Oliveira, V.
647 H., Raulund-Rasmussen, K., Sizmur, T. and Diaz, A.: Long-term acidification of
648 pH neutral grasslands affects soil biodiversity, fertility and function in a
649 heathland restoration, *Catena*, 180, 401-415, [https://doi.org/10.1016/](https://doi.org/10.1016/j.catena.2019.03.013)
650 [j.catena.2019.03.013](https://doi.org/10.1016/j.catena.2019.03.013), 2019.

651 van Dobben, H. and de Vries, W.: Relation between forest vegetation, atmospheric
652 deposition and site conditions at regional and European scales, *Environ. Pollut.*,
653 158, 921-33, <https://doi.org/10.1016/j.envpol.2009.09.015>, 2010.

654 Violle, C., Navas, M. L., Vile, D., Kazakou, E., Fortunel, C., Hummel, I., and Garnier,
655 E.: Let the concept of trait be functional!, *Oikos*, 116, 882-892, [https://doi.org](https://doi.org/10.1111/j.0030-1299.2007.15559.x)
656 [/10.1111/j.0030-1299.2007.15559.x](https://doi.org/10.1111/j.0030-1299.2007.15559.x), 2007.

657 Vitousek, P. M. and Howarth, R. W.: Nitrogen limitation on land and in the sea-how
658 can it occur?, *Biogeochemistry*, 13, 87-115, <https://doi.org/10.1007/BF00002772>,
659 1991.

660 Wang, P., Guo, J., Xu, X., Yan, X., Zhang, K., Qiu, Y., Zhao, Q., Huang, K., Luo, X.,
661 Yang, F., Guo, H., and Hu, S.: Soil acidification alters root morphology,
662 increases root biomass but reduces root decomposition in an alpine grassland,
663 *Environ. Pollut.*, 265, 115016, <https://doi.org/10.1016/j.envpol.2020.115016>,
664 2020.

665 Yang, F., Zhang, Z., Barberán, A., Yang, Y., Hu, S., Guo, H. Nitrogen-induced
666 acidification plays a vital role driving ecosystem functions: Insights from a 6-
667 year nitrogen enrichment experiment in a Tibetan alpine meadow, *Soil Biol.*
668 *Biochem.*, 153, 108107, <https://doi.org/10.1016/j.soilbio.2020.108107>, 2021.

669 Yang, G., Lü, X., Stevens, C. J., Zhang, G., Wang, H., Wang, Z., Zhang, Z., Liu, Z.,
670 and Han, X.: Mowing mitigates the negative impacts of N addition on plant
671 species diversity, *Oecologia*, 189, 769-779, [https://doi.org/10.1007/s00442-019-](https://doi.org/10.1007/s00442-019-04353-9)
672 [04353-9](https://doi.org/10.1007/s00442-019-04353-9), 2019.

673 Yang, Y., Ji, C., Ma, W., Wang, S., Wang, S., Han, W., Mohammat, A., Robinson, D.,
674 and Smith, P.: Significant soil acidification across northern China's grasslands
675 during 1980s-2000s, *Global Change Biol.*, 18, 2292-2300, [https://doi.org/10.1111](https://doi.org/10.1111/j.1365-2486.2012.02694.x)
676 [/j.1365-2486.2012.02694.x](https://doi.org/10.1111/j.1365-2486.2012.02694.x), 2012.

677 Yu, H., He, N., Wang, Q., Zhu, J., Gao, Y., Zhang, Y., Jia, Y., and Yu, G.:
678 Development of atmospheric acid deposition in China from the 1990s to the
679 2010s, *Environ. Pollut.*, 231, 182-190,
680 <http://doi.org/10.1016/j.envpol.2017.08.014>, 2017.

681 Yu, Q., Chen, Q., Elser, J. J., He, N., Wu, H., Zhang, G., Wu, J., Bai, Y., and Han, X.:
682 Linking stoichiometric homeostasis with ecosystem structure, functioning and
683 stability, *Ecol. Lett.*, 13, 1390-1399, [https://doi.org/10.1111/j.1461-0248.](https://doi.org/10.1111/j.1461-0248.2010.01532.x)
684 [2010.01532.x](https://doi.org/10.1111/j.1461-0248.2010.01532.x), 2010.

685 Zhang, B., Cadotte, M. W., Chen, S., Tan, X., You, C., Ren, T., Chen, M., Wang, S.,
686 Li, W., Chu, C., Jiang, L., Bai, Y., Huang, J., and Han, X.: Plants alter their
687 vertical root distribution rather than biomass allocation in response to changing
688 precipitation, *Ecology*, 100, e02828, <https://doi.org/10.1002/ecy.2828>, 2019.

689 [Zhang, D., Peng, Y., Li, F., Yang, G., Wang, J., Yu, J., Zhou, G. and Yang, Y.: Above-](#)
690 [and belowground resource acquisition strategies determine plant species](#)
691 [responses to nitrogen enrichment. *Ann. Bot.*, 128, 31-44, \[https://doi.org/10.1093\]\(https://doi.org/10.1093/aob/mcab032\)](#)
692 [/aob/mcab032, 2021.](#)

693 Zuchi, S., Cesco S., and Astolfi S.: High S supply improves Fe accumulation in
694 durum wheat plants grown under Fe limitation, *Environ. Exp. Bot.*, 77, 25-32,
695 <https://doi.org/10.1016/j.envexpbot.2011.11.001>, 2012.

696

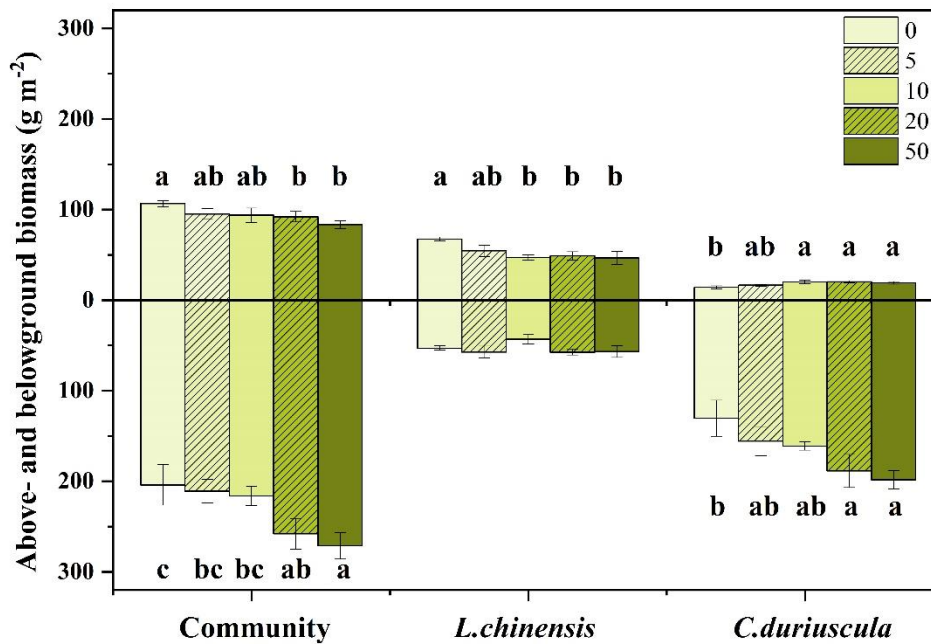
697

698

699

700

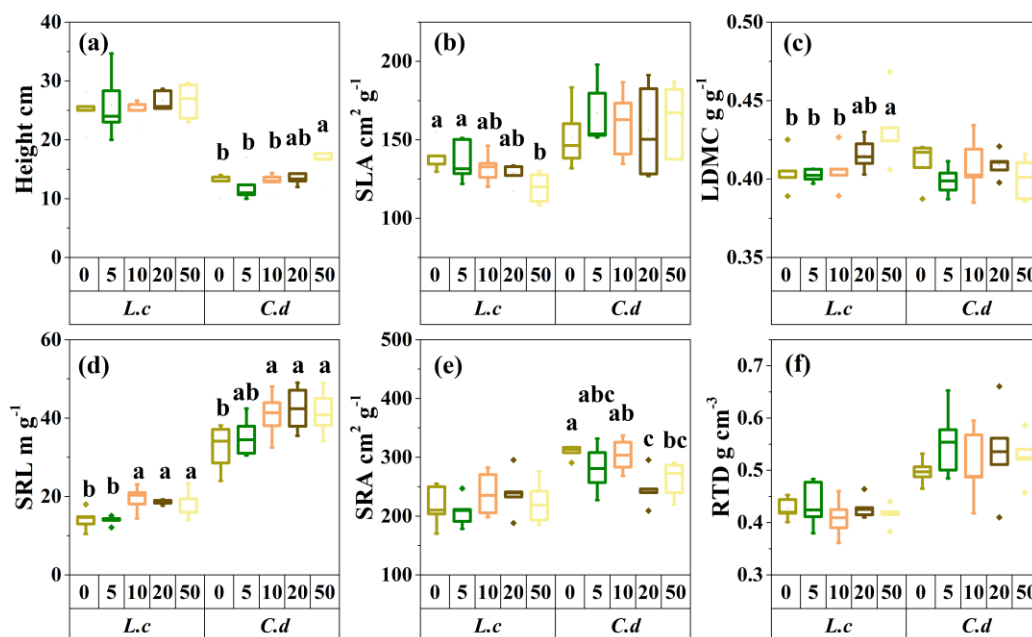
701 **Figures**



702

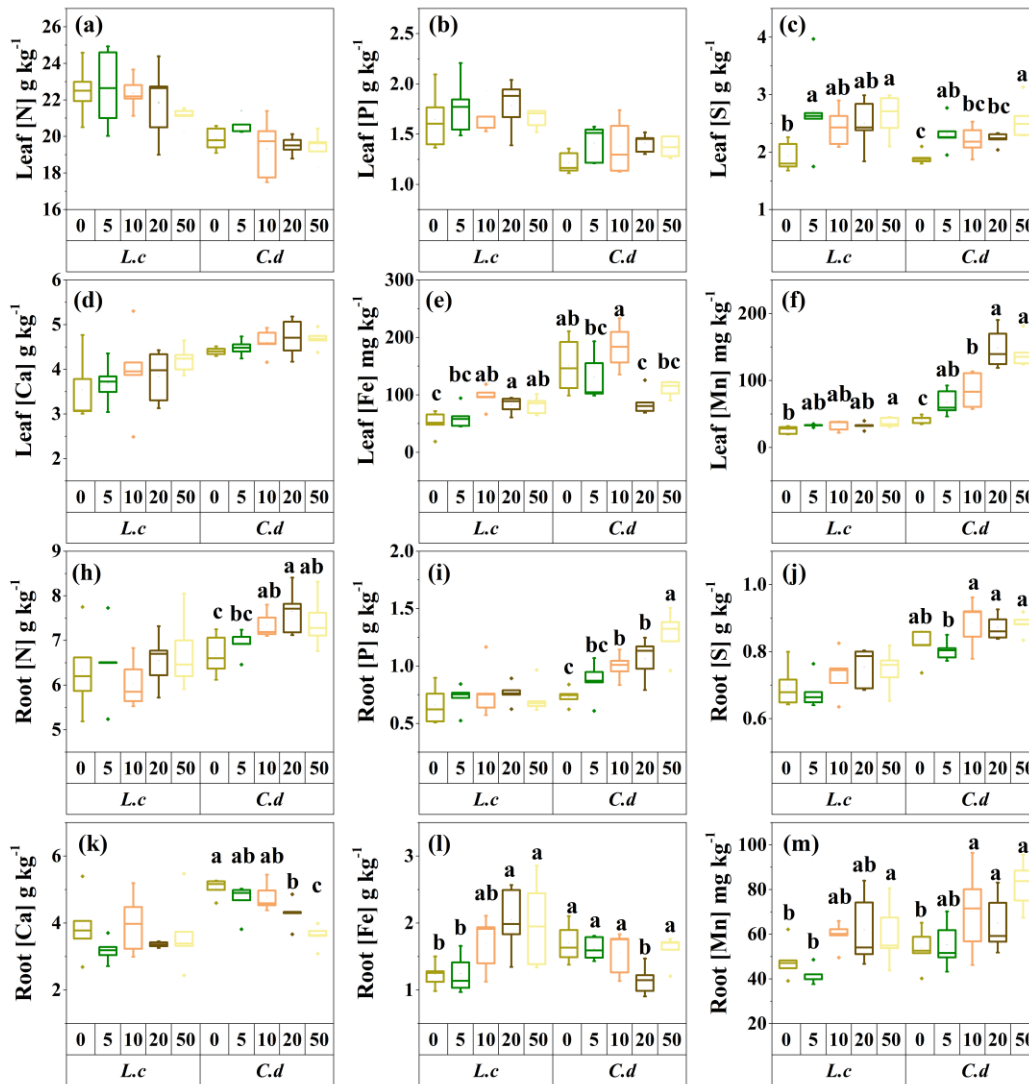
703 **Fig. 1** Effects of S addition on community and species aboveground and belowground
 704 biomass. Bars are means \pm the standard error. Lower case letters indicate significant
 705 difference among treatments ($P < 0.05$).

706



707

708 **Fig. 2** The response of the morphological traits to S addition for the two dominant
 709 species in a meadow steppe. Abbreviations: SLA, Specific leaf area; LDMC, Leaf dry
 710 matter content; SRL, specific root length; SRA, specific root area; RTD, root tissue
 711 density; *L.c.*, *L. chinensis*; *C.d.*, *C. duriuscula*. Different letters above the bars indicate
 712 significant influence among the S-addition level by one-way ANOVA at $P < 0.05$.
 713



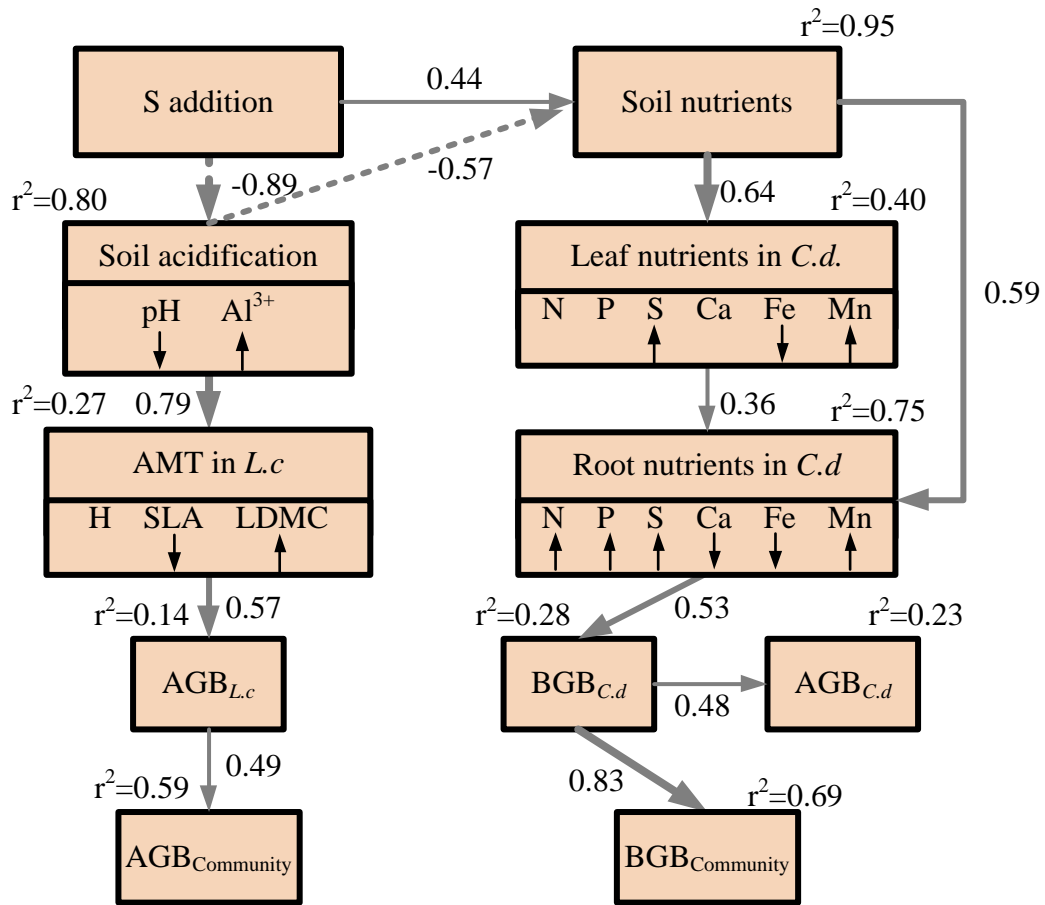
714
 715 **Fig. 3** The response of the chemical traits to S addition for the two dominant species in
 716 a meadow steppe. Abbreviations: Leaf [N], leaf N concentration; Leaf [P], leaf P
 717 concentration; Leaf [S], leaf S concentration; Leaf [Ca], leaf Ca concentration; Leaf
 718 [Fe], leaf Fe concentration; Leaf [Mn], leaf Mn concentration; Root [Ca], root Ca
 719 concentration; Root [Fe], root Fe concentration; Root [Mn], root Mn concentration;

720 Root [N], root nitrogen concentration; Root [P], root phosphorus concentration; Root
721 [S], root sulfur concentration; *L.c*, *L. chinensis*; *C.d*, *C. duriuscula*. Different letters
722 above the bars indicate significant influence among the S-addition level by one-way
723 ANOVA at $P < 0.05$.

724

725

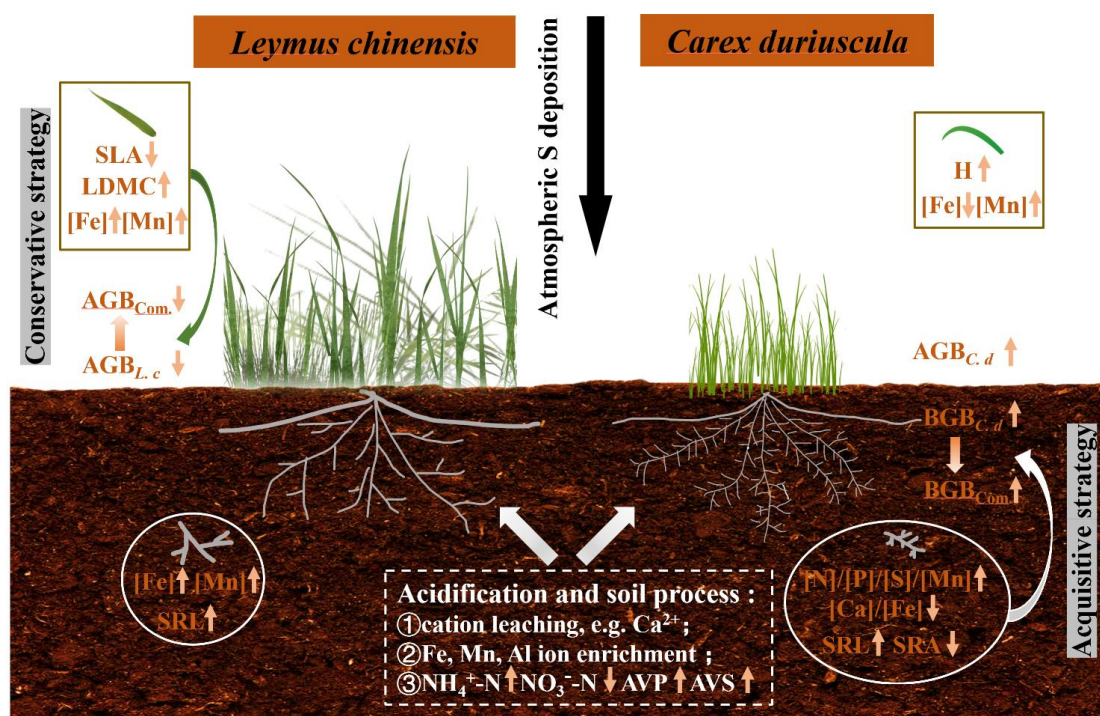
726



728

729 **Fig. 4** Structural equation model of S addition on plant community biomass through
 730 the plausible pathways. Square boxes indicate the included variables in the analysis: S
 731 addition; Soil nutrients include soil $\text{NH}_4^+\text{-N}$ and $\text{NO}_3^-\text{-N}$ concentrations, soil available
 732 phosphorus, soil available sulfur; soil exchangeable cations Ca^{2+} , Fe^{2+} and Mn^{2+} ; soil
 733 acidification includes soil pH and exchangeable Al^{3+} ; Aboveground morphological
 734 traits (AMT) includes plant height, specific leaf area, leaf dry matter content in *L.*
 735 *chinensis*; Leaf nutrients include leaf N, P, S, Ca, Fe, Mg concentrations in *C.*
 736 *duriuscula*; Root nutrients include root N, P, S, Ca, Fe, Mg concentrations in *C.*
 737 *duriuscula*; *C. duriuscula* aboveground biomass; *C. duriuscula* belowground biomass;
 738 *L. chinensis* aboveground biomass; Community aboveground biomass and
 739 belowground biomass. The symbols \downarrow and \uparrow indicate significant decrease or increase,
 740 respectively, with increasing S addition. The final SEM adequately fitted the data: $\chi^2 =$
 741 51.83, DF = 40, $P = 0.10$, AIC = 103.83, $n=25$. R^2 values next to each response variable
 742 indicate the proportion of variation explained by relationships with other variables.

743 Solid and dashed arrows represent significant positive and negative pathways ($P < 0.05$),
 744 respectively. Nonsignificant ($P > 0.05$) pathways are not shown. Values at each arrow
 745 indicate the standard path coefficient, which is equivalent to the correlation coefficient.
 746
 747



748
 749 **Fig. 5** Schematic diagram illustrating the ecological effects of S-induced soil
 750 acidification on above- and belowground biomass and traits of two **dominant** species in
 751 a meadow steppe. ↑ = increase in response to S addition; ↓ = decrease in response to S
 752 addition; Com. = Community; AVP = Soil available phosphorus; AVS = Soil available
 753 sulfur.
 754

755 **Table**

756 **Table 1** Effects of S addition on soil abiotic variables. All numbers refer to the mean
 757 (the standard error). Lower case letters indicate significant difference among treatments
 758 ($P < 0.05$).

Soil parameters	S addition				
	0	5	10	20	50
Soil pH	6.95(0.06) a	6.70(0.07) ab	6.77(0.17) a	6.17(0.31) b	5.19 (0.20) c
Ex. Al ³⁺	5.49(0.72) b	5.49(0.18) b	6.84(0.45) b	9.09(1.44) b	20.07(3.24) a
Ammonium	4.76(0.31) b	4.36(0.08) b	4.92(0.68) b	4.67(0.22) b	8.33(1.73) a
Nitrate	4.88(0.42) a	5.44(0.73) a	5.45(1.01) a	4.60(0.95) a	1.41(0.31) b
AVP	5.20(0.64) b	5.27(0.71) b	4.58(0.35) b	6.94(0.60) a	7.08(0.38) a
AVS	8.78(0.78) c	10.30(1.33) c	15.09(1.89) c	40.64(8.56) b	114.41(6.85) a
DTPA-Fe	22.10(1.14) c	27.94(0.02) bc	30.62(0.02) bc	38.07(0.04) b	58.72(0.07) a
DTPA-Mn	19.26(1.56) c	27.43(1.43) bc	33.23(3.10) bc	41.66(4.40) b	79.60(7.54) a
Ex. Ca ²⁺	22.12(0.54) a	20.66(0.90) ab	20.14(1.09) ab	19.17(0.90) b	18.50(0.61) b

759 Note: Ex. Al³⁺: Exchangeable Al³⁺, mg kg⁻¹; Ammonium: soil NH₄⁺-N concentration, mg kg⁻¹;
 760 Nitrate: soil NO₃⁻-N concentration, mg kg⁻¹; AVP: soil available phosphorus, mg kg⁻¹; AVS: soil
 761 available sulfur, mg kg⁻¹; DTPA-Fe: Soil DTPA-Fe concentration, mg kg⁻¹; DTPA-Mn: Soil DTPA-
 762 Mn concentration, mg kg⁻¹; Ex. Ca: Exchangeable Ca²⁺, cmol kg⁻¹.
 763